COBEM 2023 27TH INTERNATIONAL CONGRESS OF MECHANICAL ENGENEERING

ABCM Brazilian Society of Mechanical Sciences and Engineering
27th ABCM International Congress of Mechanical Engineering
December 04-08, 2023, Florianópolis-SC, Brazil

COB-2023-1952
EXPERIMENTS OF FLOW-INDUCED VIBRATION ON MODELS IN REGIMES OF LOW REYNOLDS NUMBERS: PART 1 – CIRCULAR-COLUMNS ARRANGEMENTS

Monique Ellen Bruner
Karen Gomes Soares
Gabriel de Paula Dittrich
André Luís Condino Fujarra
Laboratório de Interação Fluido-Estrutura – LIFE
Federal University of Santa Catarina – UFSC, Joinville / SC, Brazil
monique.bruner@posgrad.ufsc.br
karen.soares@grad.ufsc.br
gabriel.dittrich@grad.ufsc.br
andre.fujarra@ufsc.br

Abstract. *Flow-Induced Vibration (FIV) is a phenomenon that arises from the interaction between fluid flow and flexible or elastically supported structures, with consequences that must already be considered in the initial stages of the design of engineering systems affected by it. The FIV comes from the synchronization between a dominant vortex-shedding frequency and one of the natural frequencies of the system. From this synchronization, self-excited and self-controlled oscillations occur with amplitude close to the characteristic dimension of the system, which can be an isolated cylinder or arrangement of them. Exactly in this sense, the two parts of this work aim to experimentally investigate the FIV phenomenon on ultrareduced models in the Circulating Water Channel (CWC) of the LIFE-UFSC-Joinville, with a view to screening arrangements for floaters of Semi-Submersible Platforms (SSP) or Floating Offshore Wind Turbines (FOWT), considering that the promising cases can be furthermore investigated via CFD at full-scale Reynolds numbers, but also considering that, by themselves, the experimental results herein obtained already serve as validation for numerical simulation models in the same Reynolds number range. The ultrareduced models of this Part 1 are arrangements of three or four circular columns, equidistant from each other of $S = 2D$, $3D$ and $4D$ (where D is the diameter of the column), and tested according to the headings at 0, 45, 90 and 180 degrees, depending on the arrangement. All the arrangements tested had an aspect ratio $T/D = 2$ (where T is the column draft) and a reduced mass $m^* \approx 1.83$. Incident flows are characterized by low Reynolds numbers between 598 and 1318, equivalent to seven different flow velocities that essentially maintain the phenomenology of FIV, as is known. Inline and cross-flow displacements are recorded by a Motion Capture System (MCS) to determine the dimensionless amplitudes and frequencies of the FIV, using statistical and uncertainty analyses and the Fast Fourier Transform (FFT). Comparisons with results found in the literature, but at higher Reynolds numbers, reinforce that the arrangements with smaller spacing show smaller oscillation amplitudes and that the heading angle does not appreciably influence the results for the arrangements with the highest column distance. As initially proposed, therefore, it can be stated that CWC experiments with low Reynolds numbers serve as a faster and cheaper methodology for screening arrangements such as those of FOWT – the original contribution of this work.*

Keywords: *Flow-Induced Vibration (FIV), Low Reynolds Numbers, Circular-Columns Arrangements, Circulating Water Channel (CWC), ultrareduced Models, Two Degrees of Freedom*

1. INTRODUCTION

Fluid-Structure Interactions (FSI) are couplings of laws that describe fluid dynamics and structural mechanics, characterized by phenomena determined by the interactions between a structure, rigid or not, fixed or in movement, and the fluid flow, internal or external to the structure (Nakamura *et al.*, 2013).

Among many other interactions, FSI encompasses a wide range of phenomena, including vortex shedding, Flow-Induced Vibration (FIV), wave-induced motions, and hydrodynamic loads, all of which naturally depend on specific flow conditions and structural properties. In due course, it is important to note that such interactions must be considered even in the early stages of engineering system design, due to possible fatigue failures as a result of the oscillatory behavior of this scenario (Defensor Filho, 2018).

In fluid dynamics, FIV has fascinated researchers and engineers for decades. This phenomenon focuses specifically on the vibrations or oscillations induced by the fluid flow itself. FIV occurs when the fluid flow around a structure induces

unsteady flow patterns, leading to periodic variations in the forces acting on the structure. These variations can result in resonant vibrations that amplify the dynamic response of the structure. FIV is influenced by factors such as flow velocity, Reynolds number, fluid properties, and structural characteristics. Therefore, this dynamic phenomenon can have significant implications for a wide range of industries, including floating and immersed offshore systems, marine and aerospace structures, and civil infrastructure.

Although FIV has been extensively studied in various flow regimes, the behavior of structures subjected to low Reynolds flow phenomena remains a challenging area of research because of its complexity, at least in terms of performing experiments with small structures free to oscillate at very low velocities.

The Reynolds number, Re, a dimensionless parameter that characterizes the flow regime, plays a crucial role in understanding the FIV. In low Reynolds number regimes, characterized by a slow and viscous fluid motion, the effects of fluid viscosity become more pronounced (Nakamura *et al.*, 2013). The laminar flow conditions and relatively low flow velocities give rise to intricate FIV, leading to unique characteristics that differ from those observed in higher Reynolds number flows.

As mentioned, the study of FIV in low Reynolds number regimes presents a myriad of challenges. Traditional theories and models, developed primarily for high Reynolds numbers, often fail to accurately predict the dynamic behavior of structures in these regimes. The increased significance of viscous forces and the formation of slender vortical structures demand novel approaches to understanding and modeling complex FIV mechanisms in action. Understanding the phenomenon in the low Reynolds regime is not only scientifically intriguing but also vital for numerous practical applications. Offshore structures such as risers, mooring lines, and marine cables can be subjected to low Reynolds number flow conditions, particularly in regions with low flow velocities, such as near the seabed or within ice-infested waters.

Therefore, by understanding the nuances of FIV in low Reynolds number regimes, engineers and researchers can develop more accurate predictive models, design guidelines, and mitigation strategies to ensure the longevity and reliability of structures exposed to fluid-induced vibrations. Ultimately, such advancements will not only enhance the safety and efficiency of engineering systems.

Extensive research has been conducted on the flow-induced responses of cylinders, providing fundamental knowledge on vibration mechanisms, interactions, and mitigation techniques. The comprehensive understanding gained from studying cylinder vibrations serves as a valuable foundation for exploring and addressing FIV in more complex structures, such as Semi-Submersible Platforms (SSP) and Floating Offshore Wind Turbines (FOWT).

Recently, research works such as (Parameshwaran *et al.*, 2016), (Gonçalves *et al.*, 2020b) and (Gonçalves *et al.*, 2020a) relate to the FIV phenomenon for three and four columns and the influence of structural dynamics for different column spacings and geometries. Other experiments on the dynamics and structural influence of this phenomenon were considered for multicolumn systems, with four or three columns, differentiating the distances between them, such as the work by (Liu *et al.*, 2016) and (Irani *et al.*, 2015).

FOWT, for example, represents a promising frontier in the generation of renewable energy, enabling the exploitation of wind resources in deep waters. However, these floating structures face distinct challenges due to their interaction with the wind, waves, and currents. The dynamic nature of the marine environment, coupled with the flexible mooring systems of floating turbines, can lead to complex FIV phenomena. Therefore, the lessons learned from studying FIV on cylinders can be applied to the design, analysis and optimization of floating wind turbines.

By comparing FIV on cylinders and floating wind turbines, researchers and engineers can gather valuable information about the unique aspects of FIV in offshore wind applications. Understanding the underlying mechanisms, including vortex shedding, fluid-structure interaction, and wake-induced vibrations, allows the development of more accurate predictive models and efficient mitigation strategies.

The knowledge gained from studying FIV on cylinders can be applied to FOWT to enhance their performance, durability, and reliability. Lessons learned from cylinder vibrations, such as the importance of fluid-structure interaction, the effects of flow velocities and Reynolds numbers, and the role of vibration control techniques, can be adapted to address FIV challenges in floating wind turbines.

Considering this scenario, the present work experimentally investigates the foundations of the phenomenon of FIV, possibly VIV, with a view to screening ultrareduced models of floaters to support SSP or FOWT, promoting the selection of the best cases for in-depth investigations in future works via Computational Fluid Dynamics (CFD) in real-scale Reynolds numbers, in addition to the possibility that the experimental results thus obtained already serve as part of the validation for the numerical simulation models themselves in the same Reynolds number range.

The physical models in this work are arrangements of three and four circular small columns equidistant from each other, with ratios $S/D = 2$, 3 and 4, where D is the diameter of the column, tested according to headings at 0, 45, 90 and 180 degrees, depending on the arrangement. Incident flows are characterized by low Reynolds numbers $524 \leq Re \leq 1196$, equivalent to seven different velocities in the Circulating Water Channel (CWC) of the Fluid-Structure Interaction Laboratory (LIFE) at UFSC-Joinville.

2. METHODOLOGY

The experiments were carried out in the CWC at LIFE-UFSC-Joinville, with a test section of $1200mm \times 575mm$ (length $\times$ width). The flow speed control was carried out by varying the depth, which was selected to reach a Reynolds number range from 597.5 to 1317.5, as presented in Tab. 1.

Table 1. List of drafts, flow velocities, and tested Reynolds numbers of the Circular Cylinder.

Water depth (mm)	Velocity (m/s)	Reynolds number
150	0.0527	1317.5
175	0.0445	1112.5
200	0.0374	935.0
225	0.0329	822.5
250	0.0302	755.0
275	0.0260	650.0
300	0.0239	597.5

All experimental arrangements were subjected to the same seven uniform flow velocities U. The range was selected considering the VIV resonance interval known from the literature, $4 < Vr < 10$, naturally taking as a reference the behavior of the single circular cylinder investigated in Bruner *et al.* (2023).

Figure 1 shows the experimental apparatus composed of a model, the elastic support (responsible for equally restoring forces in cross-flow and inline directions), the CWC, and the Motion Capture System (MCS) – an OptiTrack device, which comprises a data acquisition and conditioning system managed by the Motive program, an Esync synchronizer and three targets attached to the model. More details about this experimental setup can also be found in Bruner *et al.* (2023).

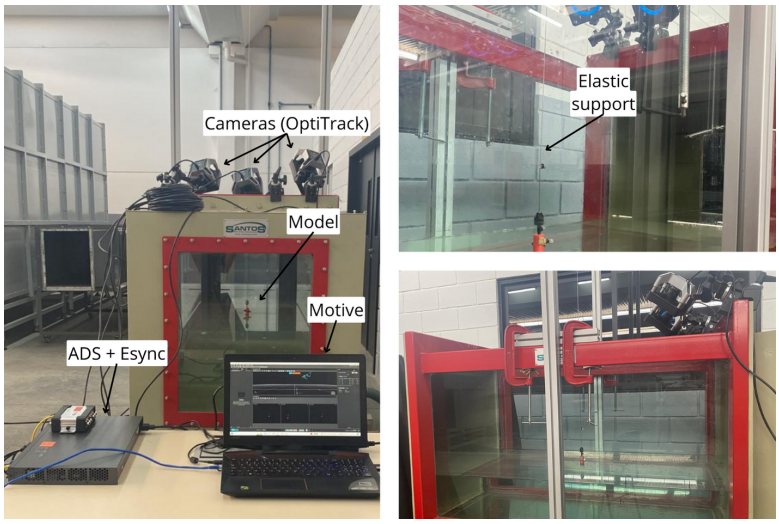

Figure 1. Experimental set-up used to perform the experiments.

The models were 3D printed with PLA filament and ballasted in all the arrangements having the same mass ratio $m^* = 1.83$. Circular columns have the same outer diameter of $20mm$ and an immersed aspect ratio of $AR = 2$. In total, six arrangement models were printed, with sets of 3 or 4 columns equidistant from each other, in ratios of $S/D = 2$, 3, and 4. The models for each arrangement considered can be seen in Figure 2).

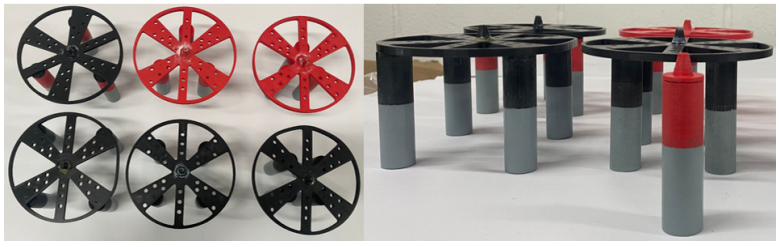

Figure 2. Small-scale models of the circular cylinder arrangements.

The four-column arrangements were subjected to two different headings, of 0° and 45°. For the three-column arrangement, three headings were considered, namely 0° 90° and 180°. Figure 3 shows all arrangements in relation to flow velocity U.

Figure 3. Illustration of the headings for each arrangement considering the flow incidence denoted by U.

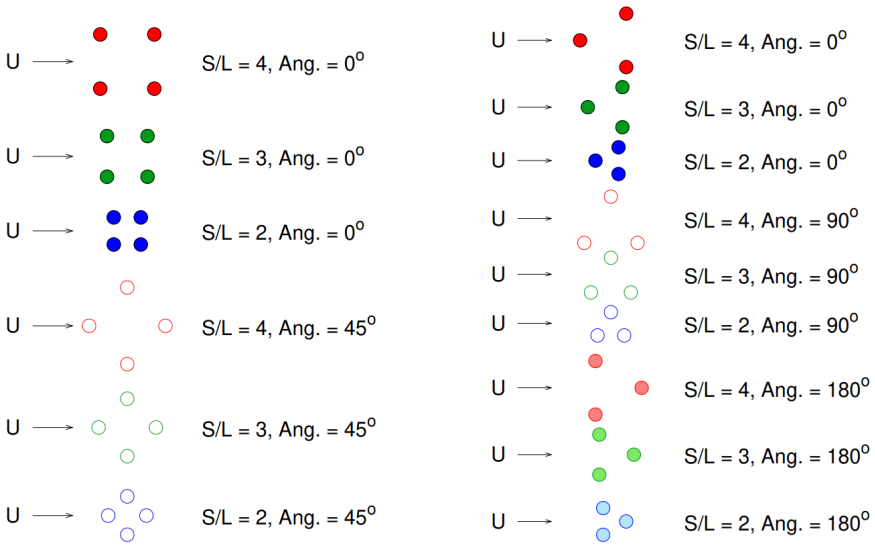

According to the guidelines for Vortex Induced Motion (VIM) tests proposed by the *International Towing Tank Conference* (ITTC, 2021), at least 20 complete FIV cycles must be recorded, at a frequency of acquisition at least 10 times greater than the highest frequency of interest, Note that each arrangement has its natural frequency f_n, which implies slightly different ranges of reduced velocity as described in the Equation 1.

$$Vr = \frac{U_x}{fn_y \cdot D} \tag{1}$$

For FIV tests carried out in this work, each arrangement-heading-spacing-velocity combination was tested considering 3 repetitions of 5 minutes in each acquisition, which is enough time for at least 60 cycles of the phenomenon to be registered. Therefore, the complete matrix of experiments totals 315 runs, as can be concluded from Tab. 2.

Table 2. Matrix of 105 tests repeated three times each.

Number of columns	Angle of attack	S/D	Reduced velocity, Vr	$f_n(Hz)$
3	0°	2	4.44 ; 4.83 ; 5.35 ; 6.12 ; 6.95 ; 8.27 ; 9.80	0.27
3	90°	2	4.44 ; 4.83 ; 5.35 ; 6.12 ; 6.95 ; 8.27 ; 9.80	0.27
3	180°	2	4.44 ; 4.83 ; 5.35 ; 6.12 ; 6.95 ; 8.27 ; 9.80	0.27
4	0°	2	4.51 ; 4.91 ; 5.43 ; 6.21 ; 7.06 ; 8.40 ; 9.94	0.26
4	45°	2	4.51 ; 4.91 ; 5.43 ; 6.21 ; 7.06 ; 8.40 ; 9.94	0.26
3	0°	3	4.53 ; 4.92 ; 5.45 ; 6.23 ; 7.08 ; 8.43 ; 9.98	0.26
3	90°	3	4.53 ; 4.92 ; 5.45 ; 6.23 ; 7.08 ; 8.43 ; 9.98	0.26
3	180°	3	4.53 ; 4.92 ; 5.45 ; 6.23 ; 7.08 ; 8.43 ; 9.98	0.26
4	0°	3	4.69 ; 5.10 ; 5.65 ; 6.45 ; 7.33 ; 8.73 ; 10.33	0.25
4	45°	3	4.69 ; 5.10 ; 5.65 ; 6.45 ; 7.33 ; 8.73 ; 10.33	0.25
3	0°	4	4.54 ; 4.94 ; 5.48 ; 6.25 ; 7.11 ; 8.46 ; 10.02	0.26
3	90°	4	4.54 ; 4.94 ; 5.48 ; 6.25 ; 7.11 ; 8.46 ; 10.02	0.26
3	180°	4	4.54 ; 4.94 ; 5.48 ; 6.25 ; 7.11 ; 8.46 ; 10.02	0.26
4	0°	4	4.63 ; 5.04 ; 5.58 ; 6.38 ; 7.25 ; 8.62 ; 10.21	0.26
4	45°	4	4.63 ; 5.04 ; 5.58 ; 6.38 ; 7.25 ; 8.62 ; 10.21	0.26

As mentioned, data acquisition took place through the OptiTrack MCS. Three cameras were installed downstream of the CWC. The cameras tracked the rigid body movements by means of 3 reflective targets attached to the models. This first data processing takes place within a system-specific program called Motive, which at the end recorded a “CSV-file”. The acquisition frequency used was 100Hz, much higher than the expected frequencies, which are around $0.3Hz$.

The time histories of the cross-flow and inline displacements were analyzed using computational routines in the GNU-Octave environment. Routines evaluate the signals and then select peaks and troughs (extreme values). Then they calculate the absolute value of these maxima and minima, sort them in descending order, and finally calculate the mean of the 10-percent-largest values.

Therefore, dimensionless response amplitudes $A_x^{10\%}/D$ and $A_y^{10\%}/D$ are considered based on the mean of the 10-percent-largest values, taking the diameter of a column as a reference. The results also consider the three repetitions for each arrangement.

In terms of frequency, the analyzes were performed by using the Fast Fourier Transform (FFT), and the dominant frequency of movements was considered to be the highest spectral peak in the Power Spectrum Density (PSD) graph. As in the notation commonly found in the literature, the dominant frequencies are presented in a dimensionless form, given by their relation to the transverse natural frequency obtained in water, $f_{ny} = f_n$.

3. RESULTS AND DISCUSSIONS

Analyzes of FIV acting on the three- and four-column arrangements include a thorough examination of the dimensionless amplitudes and frequencies of the inline and cross-flow directions, providing information on the dynamic behavior of the models under investigation. In addition, they explore the influence of key parameters such as reduced velocity, Reynolds number, and structural properties on the observed vibration characteristics.

Figure 4 shows examples of time histories in both X and Y directions of a four-column arrangement, at the reduced velocity where the VIV peak occurs. The time history response provides a dynamic depiction of the structural oscillations experienced by a system subjected to fluid flow. Allows for inspecting the influence of key parameters, such as flow velocity and structural properties, on the time-varying response characteristics for high reduced velocity.

The vibration patterns are consistent with the well-documented features of VIV, in which fluid flow induces vortex shedding, leading to cyclic forces acting on the structure and driving its oscillatory response. The observed regularity and periodicity in the time history data strongly corroborate the manifestation of VIV in the low Reynolds regimes tested here.

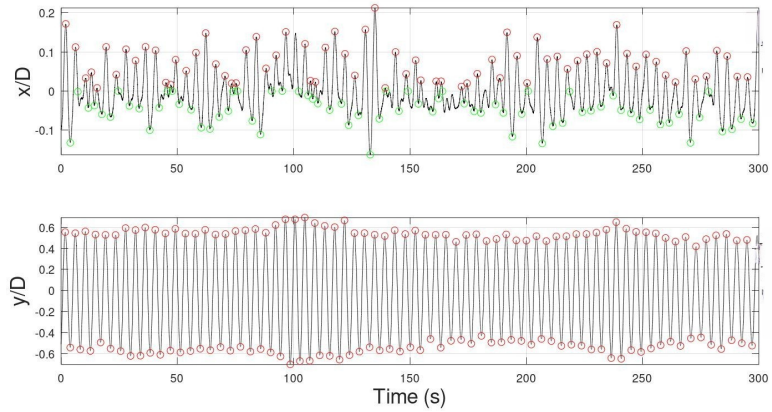

Figure 4. Examples of displacement time histories for the four-column arrangement in $\theta = 45°$and $Vr = 4.63$.

Figure 5 illustrates the response amplitudes of cross-flow vibrations. The vertical axis denotes the dimensionless amplitude $A_y^{10\%}/D$ based on the ratio between the mean value and the diameter of the system. The horizontal plane denotes the spacing ratio between columns ($S/D = 2$, 3, and 4) by the reduced velocities tested.

For most of the velocities tested, and regardless of the flow incidence, arrangements with a spacing $S/D = 4$ have higher response amplitudes in the cross-flow direction, Figure 5 (a) and (b). This graph exhibits a notable peak of amplitude at a reduced velocity of approximately 9. In both angles, a second peak can be seen at $Vr \approx 7$.

Moreover, the response amplitudes $A_y^{10\%}/D$ for $S/D = 3$ are intermediate between $S/D = 2$ and 4. The peak occurs at $Vr \approx 7$ at both angles, but for $\theta = 45°$ this amplitude the reduction is more prominent at higher velocities. In general, the flow incidence angle is significant at higher reduced velocities, at least in terms of the amplitude of the cross-flow response.

The four-column arrangements with $S/D = 2$ show amplitudes significantly lower than the others, at least in a lower range of reduced velocities. At 45°of incidence, an amplitude peak can be observed in Figure 5 (b), and its behavior can be due to an interaction between neighboring cylinders. In a column arrangement, the wakes from neighboring cylinders can interact with each other, leading to complex flow patterns. These interactions can cause fluctuations in the forces acting on the arrangement, resulting in the observed behavior.

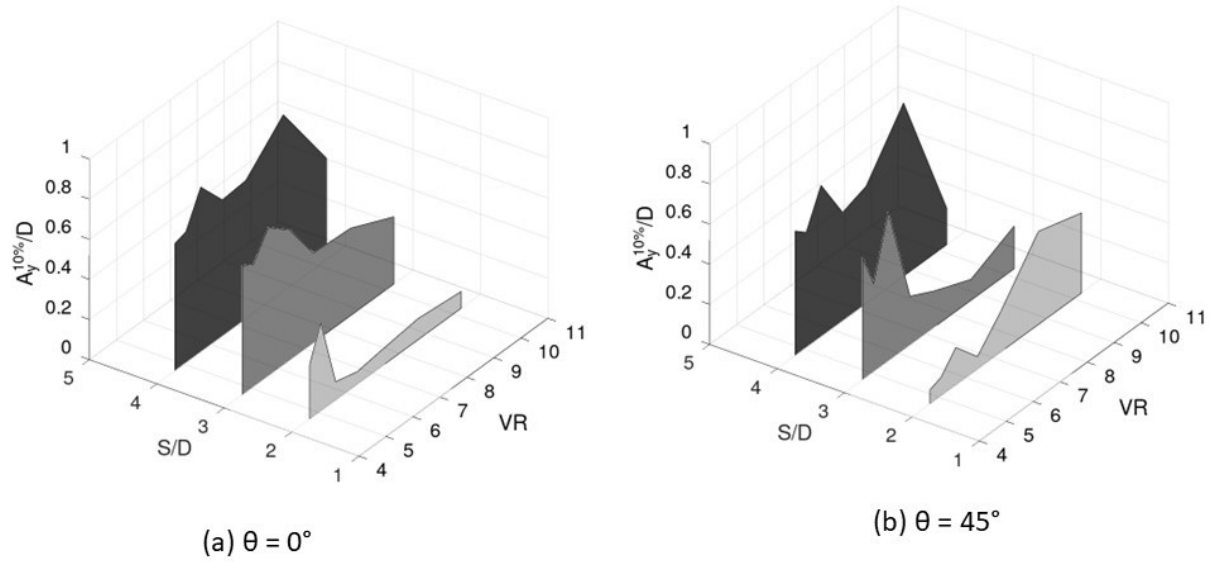

Figure 5. Dimensionless amplitudes of cross-flow vibrations $A_y^{10\%}/D$ for the four-column arrangements, as a function of the distances S/D and reduced velocities Vr.

Figure 6 shows the response amplitudes of the cross-flow vibrations. The spacing in a three-column arrangement plays a crucial role in influencing the VIV phenomenon. Smaller column spacing tends to enhance the interaction between neighboring cylinders, leading to synchronization effects. This synchronization can result in amplified vibrations and larger amplitudes throughout the arrangement.

Additionally, a smaller column spacing seems to promote mode coupling, where the vibrations of one cylinder influence or excite the vibrations of nearby cylinders. This coupling of vibration modes can alter the response frequencies and amplitudes of FIV. Figure 6 shows this behavior clearly, the arrangement with $S/D = 2$ has larger amplitudes compared to the other two relative distances and the angle of incidence does not influence the dynamic response. In other words, the flow incidence has little influence on the magnitude of the response for the highest reduced velocities, so it can be assumed that the columns are close enough for the entire arrangement to behave as a single cylinder.

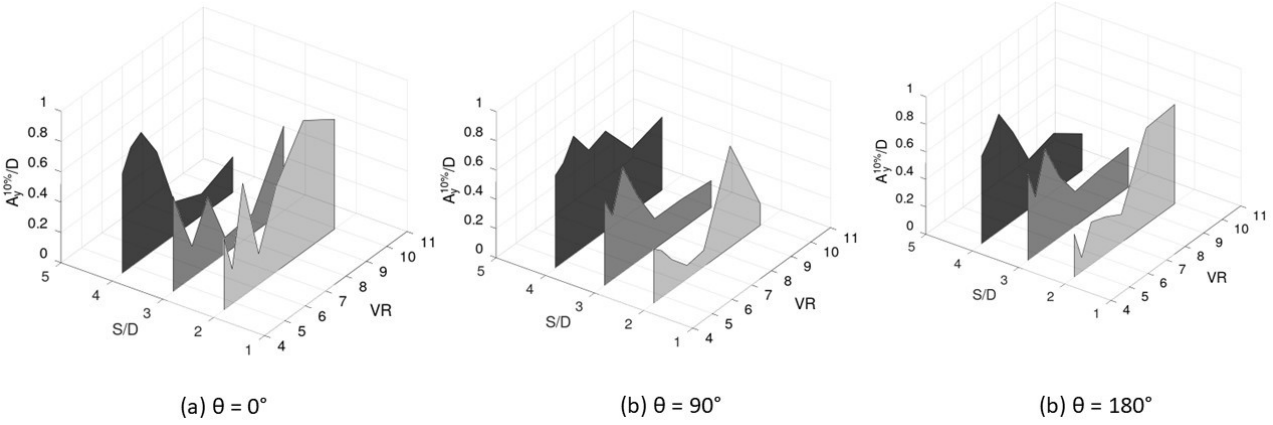

Figure 6. Dimensionless amplitudes of cross-flow vibrations $A_y^{10\%}/D$ for the three-column arrangements, as a function of the distances S/D and reduced velocities Vr.

However, a larger column spacing probably results in a reduced interaction between the shedding vortices, which may lead to a decrease in the synchronization effects and a more isolated response for each column. Larger spacing can also affect the shedding frequency and vortex formation, potentially influencing the dominant frequencies and amplitudes of the FIV response.

Figure 7 shows the response amplitudes of the inline vibrations $A_x^{10\%}/D$ for the incidence angle tested with the three-column and four-column arrangement. As expected, these experimental findings show a notable disparity in the

response amplitudes between the inline and cross-flow directions. The data clearly indicate that the amplitudes in the inline direction $A_x^{10\%}/D$ are consistently lower than those in the cross-flow direction $A_y^{10\%}/D$. This disparity can be attributed to several influential factors; among them, a higher flow velocity in the inline direction results in more vigorous shedding of vortices, and subsequently in greater energy dissipation. As a consequence, the amplitudes of vibrations induced by vortex shedding tend to be diminished in the inline direction.

At a spacing ratio of $S/D = 3$, the interaction between the columns appears to alter the shedding patterns, shedding frequencies, and the entire flow field around the downstream cylinders. This influence is reflected in the amplitude and frequency of inline vibrations compared to the single-cylinder scenario. These hypotheses offer plausible insights for further conducting Particle Image Velocimetry (PIV) experiments and/or CFD simulations.

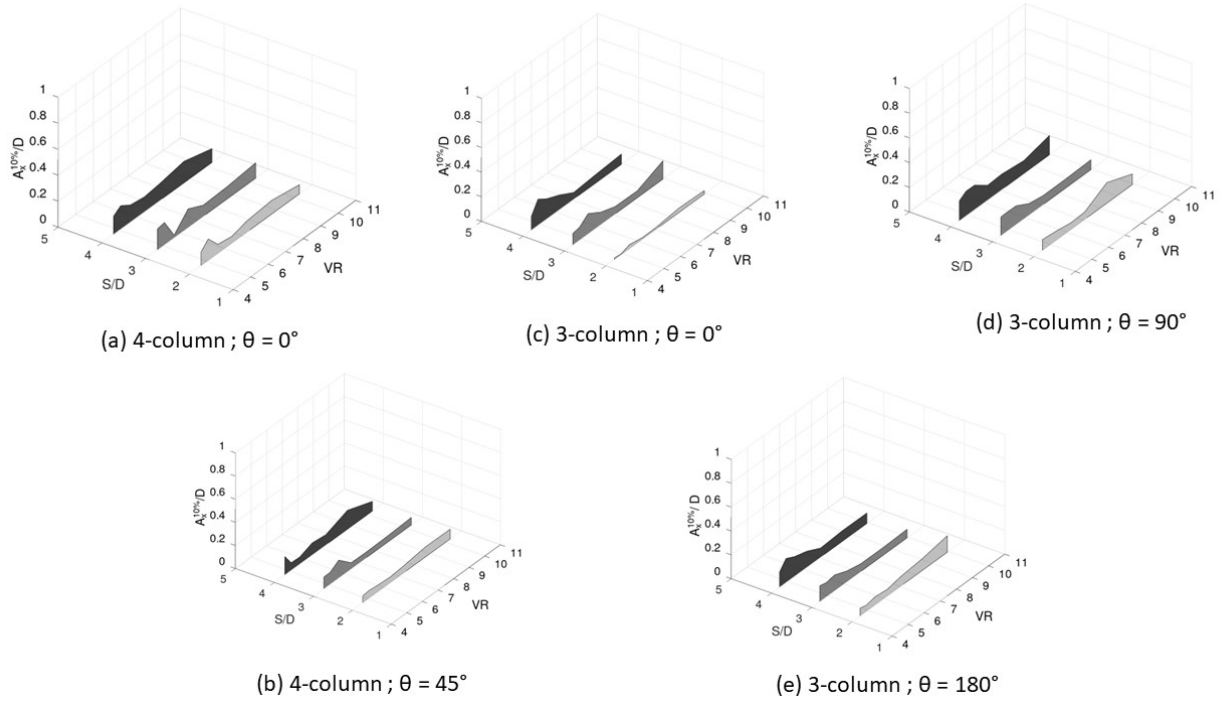

Figure 7. Dimensionless amplitudes of inline vibrations $A_x^{10\%}/D$ for the three and four-column arrangements, as a function of the distances S/D and reduced velocities Vr.

Figures 8 and 9 show dimensionless frequencies denoted by $f_x^* = f_x/f_n$ and $f_y^* = f_y/f_n$. When a cylinder oscillates in fluid, such as water or air, it experiences added mass and added damping effects. These effects alter the natural frequency of the cylinder compared to its natural frequency. The effect of added mass is the result of changes in the near-pressure field, increasing the effective mass considered for the dynamics.

Regarding the inline direction, Figure 8 shows that the angle of incidence does not influence the frequency ratio for the four-column arrangement. With respect to the three-column arrangement, the angle of incidence shows an influence on the results, especially with the arrangement with smaller spacing. These results can be justified by the proximity of the columns and, by that, the system behaves like a single body with a different geometry when struck by current.

Similarly, Figure 9 shows the same characteristics for f_y^*. Most combinations between arrangements and spacing showed that the angle of incidence does not reflect changes in the values of the frequency ratio of the system. However, especially for the arrangement of four columns and smaller spacing, this angle had a significant impact on the response in terms of frequency, mainly for the higher reduced velocities.

Combining the low frequency and low amplitude for the case of the four-column arrangement and smaller spacing, it can be said that it is a dynamic that is often characterized by smooth and elongated oscillations that do not exert significant force or impact on the floater model. This can be an indication of a similar arrangement in SSP and/or FOWT, at least concerning the FIV phenomena investigated herein.

The analysis of the results demonstrates that the systems studied exhibit a vibration of high amplitude and low frequency in FIV. This particular behavior has significant implications for marine structures. The high amplitude of the vibrations indicates substantial displacements and movements, which can lead to increased stresses and fatigue on the mooring lines. Furthermore, the low-frequency nature of vibrations can contribute to prolonged exposure to these dynamic loads. The combination of high-amplitude and low-frequency vibrations can pose challenges in terms of structural integrity.

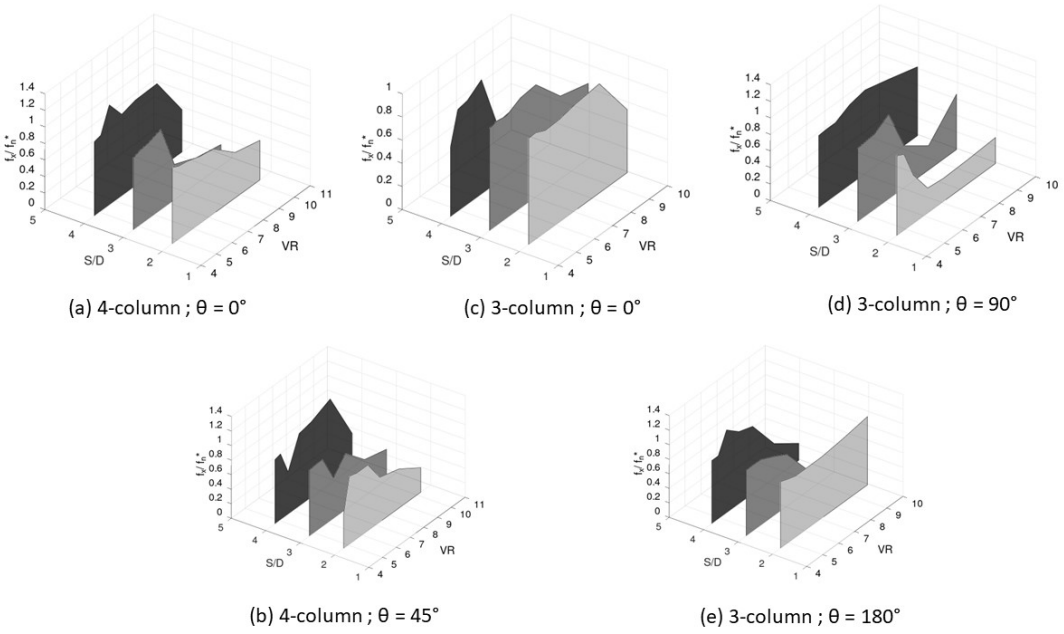

Figure 8. Dimensionless frequencies of inline vibrations f_x^* for the three and four-column arrangements, as a function of the distances S/D and reduced velocities Vr.

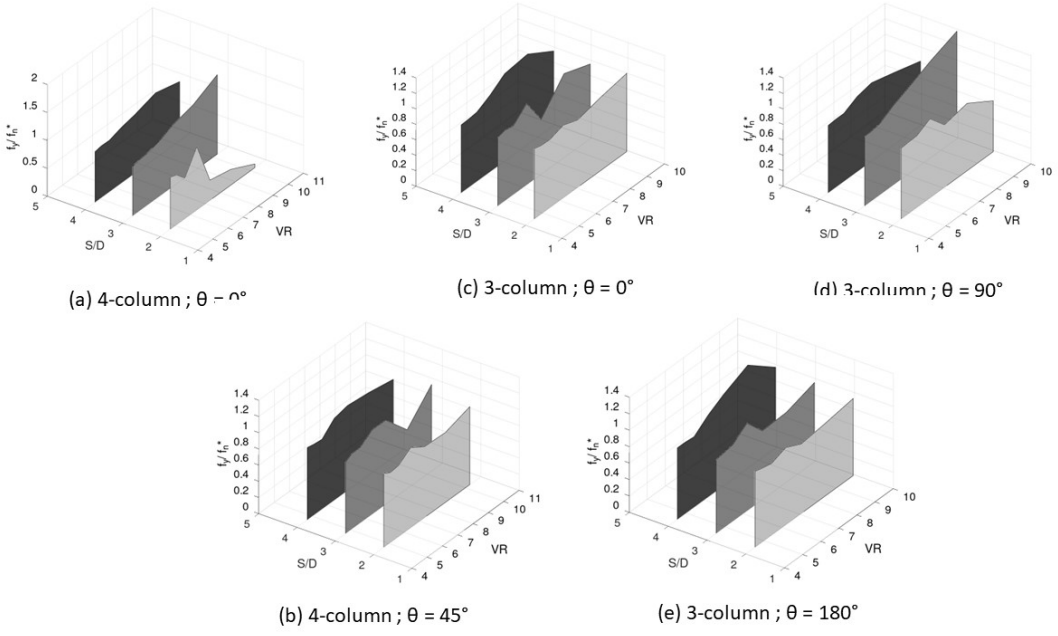

Figure 9. Dimensionless frequencies of cross-flow vibrations f_y^* for the three and four-column arrangements, as a function of the distances S/D and reduced velocities Vr.

4. CONCLUSIONS

Since testing full-scale prototypes is unfeasible due to the enormous dimensions and costs of the mentioned systems, and experiments with medium-sized models are still expensive and challenging to manipulate experimentally, even smaller-scale models were built with a diameter of $20mm$ using 3D printing in PLA. These models had an aspect ratio of 2, which means that their submerged portion corresponded to two diameters. The relative distances between the columns were varied, with values of S/D equal to 2, 3, and 4.

In addition to the variation in column spacing, the angle of flow incidence was also varied. For the three-column arrangements, the angles tested were 0°, 90°, and 180°, while for the four-column arrangements, the angles tested were

0°and 45°. Seven test velocities were examined, covering a range of reduced velocities from 4.44 to 10.33. It is worth noting that the arrangements consist of columns interconnected and supported by elastic support allowing them the freedom to oscillate on the free surface in the two degrees of freedom (2DOF), inline and cross-flow, respectively, denoted as X and Y directions.

Regarding the four-column arrangements, those with larger spacing, $S/D = 3$ and 4, presented dimensionless transverse response amplitudes higher than the other arrangement, located in higher reduced velocity values, $8 < V_R < 10$, which is explained by the lower natural frequencies. This increase in response can be explained by the wake effects produced by the upstream cylinders. The lowest dimensionless amplitudes in cross-flow direction were for the $S/D = 2$, for 0°of flow incidence.

Comparing all the results obtained, it can be noticed that the behavior of arrangements with three columns is similar to the behavior of four columns. Both, despite having different configurations, responded similarly. That is, for both cases, it is noted that from $S/D = 3$, the distance between columns does not have a significant impact on the FIV amplitudes. Furthermore, the arrangements with greater spacing respond with transverse amplitudes greater than the single cylinder in their synchronization range which is located at $Vr > 7.5$. Arrangements of $S/D = 2$ responded with substantially smaller response amplitudes in both directions.

The originality of this work, therefore, lies mainly in investigating the phenomenon of FIV at low Reynolds numbers for arrangements of cylinders free to oscillate in 2dof. From the literature review carried out, the results presented here bring apparent novelty with regard to its theme. In addition, based on these results, it is not only possible to quickly and cheaply screen the best arrangements within a large range of possibilities, but also to obtain a set of values and discussions that are robust enough to be used as validation for the approaches' numerical values via computational fluid dynamics. As far as it can be ascertained prior to the present work, the numerical results with column arrangements at low Reynolds numbers did not have any other form of validation, except through indirect comparisons with experimental results of single cylinders.

5. ACKNOWLEDGEMENTS

This study was funded by the National Council for Scientific and Technological Development (CNPq), finance code 437114/2018-0. The last author also thanks CNPq for the individual research grant, code 314057/2021-8.

6. REFERENCES

Bruner, M.E., Soares, K.G., Teixeira, F.R., Fujarra, A.L.C. and Cenci, R., 2023. "Circulating water channel for investigations of fluid-structure interactions in low reynolds numbers". In *Proceedings of the 27th International Congress of Mechanical Engineering - COBEM 2023*. Florianópolis, Brazil.

Defensor Filho, W.A., 2018. *Investigação experimental de vibrações induzidas por escoamento em cilindros flexíveis com rigidez ortotrópica*. Mestrado em engenharia engenharia naval e oceânica, Universidade de São Paulo, São Paulo.

Gonçalves, R., Chame, M.E.F., Hannes, N.H., de Paula Lopes, P.P.S., Hirabayashi, S. and Suzuki, H., 2020a. "FIM – flow-induced motion of three-column platforms". *International Journal of Offshore and Polar Engineering*, Vol. 30, No. 2, pp. 177–185.

Gonçalves, R., Hannes, N.H., Chame, M.E., Lopes, P.P., Hirabayashi, S. and Suzuki, H., 2020b. "FIM - flow-induced motions of four-column platforms". *Applied Ocean Research*, Vol. 95.

Irani, M., Jennings, T., Geyer, J. and Krueger, E., 2015. "Some aspects of vortex induced motions of a multi-column floater". In *Proceedings of the ASME 2015 34th International Conference on Ocean, Offshore and Arctic Engineering*. Ocean, Offshore and Arctic Engineering Division, Canada.

ITTC, 2021. "7.5-02-07-03.13: Guideline for vim testing". International Towing Tank Conference.

Liu, M., Xiao, L., Lu, H. and Shi, J., 2016. "Experimental investigation into the influences of pontoon and column configuration on vortex-induced motions of deep-draft semi-submersibles". Vol. 123, No. 1, pp. 262–277.

Nakamura, T., Kneko, S., Inada, F., Kato, M., Ishihara, K., Nishihara, T., Mureithi, N.W. and Langthjem, M.A., 2013. *Flow-Induced Vibrations: Classifications and Lessons from Practical Experiences*. Elsevier Ltd., 2nd edition.

Parameshwaran, R., Dhulipalla, S.J. and Yendluri, D.R., 2016. "Fluid-structure interactions and flow induced vibrations: A review". *Procedia Engineering*, Vol. 144, pp. 1286 – 1293. International Conference on Vibration Problems 2015.

7. RESPONSIBILITY NOTICE

The authors are solely responsible for the printed material included in this paper.